Journal of the Korean Ceramic Society
Vol. 38, No. 12, pp. 1075~1079, 2001.

R-Curve Behavior of Silicon Carbide - titanium Carbide Composites

Hyun-Gu An and Young-Wook Kim†

Department of Materials Science and Engineering, The University of Seoul, Seoul 130-743, Korea
(Received October 15, 2001; Accepted November 26, 2001)

ABSTRACT

The R-curve for in situ-toughened SiC-30 wt% TiC composites was estimated by the indentation-strength method and compared to that of monolithic SiC with toughened microstructure. Both materials exhibited rising R-curve behavior. The SiC-TiC composites, however, displayed better damage tolerance and higher resistance to crack growth. Total volume fractions of SiC key grains, which take part in toughening mechanisms such as crack bridging and crack deflection, were 0.607 for monolithic SiC ceramics and 0.614 for SiC-TiC composites. From the microstructural characterization and the residual stress calculation, it was inferred that this superior performance of SiC-TiC composites can be attributed to stress-induced microcracking at heterophase (SiC/TiC) boundaries and some contribution from crack deflection by TiC grains.

Key words : Composites, Mechanical properties, Microstructure, SiC-TiC

1. Introduction

Many ceramics demonstrate increasing fracture toughness with increasing crack length.[1-5] This R-curve behavior arises because of the interactions of the microstructure behind the crack tip in the wake region. Specifically, on nontransforming systems such as silicon nitride[3-5] and in-situ toughened silicon carbide,[6,7] the R-curve derives from the development of a zone of bridging grains behind the crack tip, which reduces the near-tip driving force and retards subsequent crack extension. It has also been shown that some particulate composite materials such as SiC-TiB_2[8] and Si_3N_4-TiN[9] exhibit R-curve behavior.

Recently, a new SiC-TiC composite with in situ-toughened microstructure, consisted of uniformly distributed elongated α-SiC grains, equiaxed TiC grains and an amorphous grain boundary phase, has been developed from β-SiC and TiC powders with the liquid-forming additives of Al_2O_3 and Y_2O_3 by hot-pressing and subsequent annealing[10] or pressureless sintering.[11] The SiC-TiC composites had a short-crack fracture toughness of 6.0 MPa · $m^{1/2}$. This improved fracture toughness was attributed to crack bridging and deflection by elongated α-SiC grains. As a result of these toughening mechanisms, this in situ-toughened SiC-TiC composites would be expected to have rising R-curve behavior and excellent flaw tolerance.

In the present study, the R-curve behavior of SiC-30 wt% TiC composites was investigated using the indentation-strength method and was compared to that of monolithic SiC with toughened microstructure, which is known as a typical R-curve material.[6,7] The microstructure of hot-pressed and subsequently annealed SiC-30 wt% TiC composites consisted of uniformly distributed elongated SiC grains, relatively equiaxed TiC grains and an amorphous grain boundary phase.[10] The hot-pressed and subsequently annealed monolithic SiC had an unimodal microstructure consisting of elongated SiC grains and an amorphous grain boundary phase.[7] Microstructure analysis, indentation load-strength analysis (strength measured as a function of indentation load), and crack-wake observation were used to correlate the R-curve with the microstructure.

†Corresponding author : ywkim@uoscc.uos.ac.kr

2. Experimental Procedure

Commercially available α-SiC (A-1 grade, Showa Denko, Tokyo, Japan), β-SiC (Ultrafine grade, Ibiden Co., Ltd, Nagoya, Japan) and TiC (C.A.S. grade, H. C. Starck, Berlin, Germany) powders were used as the starting powders. The mean particle sizes of the α-SiC, β-SiC, and TiC powders were 0.45 μm, 0.27 μm, 1.40 μm, respectively. The α-SiC powder was added as seeds for grain growth. Two batches of powder (see Table 1) were ball-milled in ethanol with SiC grinding balls for 24 h. The milled slurry was dried and hot-pressed at 1820°C for 1 h with 25 MPa of applied pressure under argon. The hot-pressed samples were subsequently annealed at 1930°C for 0.25 h (monolithic SiC) or 4 h (SiC-30 wt% TiC composites) with 25 MPa of applied pressure under argon to enhance the grain growth and the β→α

Table 1. Batch Composition

Sample	Composition (wt%)
SiC	89% β-SiC + 1% α-SiC + 4.3% Al_2O_3 + 5.7% Y_2O_3
SiC-TiC	59.4% β-SiC + 0.6% α-SiC + 30% TiC + 4.3% Al_2O_3 + 5.7% Y_2O_3

Table 2. Characteristics of Monolithic SiC and SiC-30 wt% TiC Composites

Sample	Relative density (%)	Young's modulus (GPa)	Flexural strength (MPa)	Fracture toughness (MPa · $m^{1/2}$)	Crystalline phase	
					Major	Trace
SiC	98.3	430	495	5.3	α-SiC	β-SiC, YAG
SiC-TiC	98.9	450	424	6.2	α-SiC, TiC	β-SiC, YAG

†$Y_3Al_5O_{12}$ (yttrium aluminum garnet)

phase transformation of SiC. The annealing times for each material (ie., 0.25 h for monolithic SiC and 4 h for SiC-TiC composites) were chosen to produce a similar grain size of SiC grains in both materials.

Densities were measured using the Archimedes method. The theoretical densities of the specimens, 3.308 g/cm^3 for the monolithic SiC and 3.707 g/cm^3 for the SiC-30 wt% TiC composites, were calculated according to the rule of mixtures. Crystalline phases in the sintered specimens were determined by X-Ray Diffractometry (XRD). The sintered specimens were cut and polished, then etched with a plasma of CF_4 containing 7.8% O_2. The microstructures were observed by scanning electron microscopy (SEM). The diameter, thickness, and aspect ratio of each grain in the annealed materials have been measured using image analysis (Image-Pro Plus, Media Cybernetics, Maryland, U.S.A.), according to a procedure shown in previous studies.[12,13] The diameter of each grain (d) was determined directly from the shortest grain dimension in its two-dimensional image; the apparent length of each grain (L) was obtained from the largest dimension. The mean value of the observed aspect ratio (L/d) was considered to be an average aspect ratio. Grains considering to be an effective contributor to the toughening are defined as key grains.[12] Detailed description of the image analysis has been given in previous papers.[12,13] A total of 800 to 1100 grains was used for statistical analysis of each specimen. The grain-diameter distribution and aspect-ratio distribution for each material were obtained. The frequency distribution was expressed in terms of the percentage of the total area occupied by grains of the same diameter size. An areal percent in a two-dimensional observation approximately corresponds to volume percent in a three-dimensional observation.[14]

Specimens for R-curve test were cut into 3 mm × 2.5 mm × 25 mm bars and polished up to 1 μm finish. Prior to indentation, a thin film of gold was deposited on the indentation surface for accurate observation of the crack size and a drop of moisture-free silicon oil was spread over the site of the indentation for minimizing moisture-assisted subcritical crack growth of as-indented cracks. Special care was taken to orient the radial cracks generated from the indentation parallel to the sides of the bar. Three Vickers indentations with loads ranging from 1.96 to 294 N were made 3 mm apart in the centre of the prospective tensile surface of each test piece. A total of 32 indented bars for each of monolithic SiC and SiC-30 wt% TiC composites were directly fractured using four point bending with an inner and outer span of 10 and 20 mm, respectively. Every specimen was checked to ensure that fracture was initiated from the indent. The average strength data obtained from the specimens that fractured from the indented sites were used for the subsequent R-curve analysis as described by Krause.[15]

3. Results and Discussion

3.1. Microstructure

The characteristics of annealed materials are summarized in Table 2. The relative densities of monolithic SiC and SiC-30 wt% TiC composites were 98.3% and 98.9%, respectively. SEM micrographs of polished and etched surfaces are shown in Fig. 1. As shown, monolithic SiC had an in situ-toughened microstructure consisting of elongated α-SiC grains. The SiC-30 wt% TiC composites also had an in situ-toughened microstructure consisting of uniformly distrib-

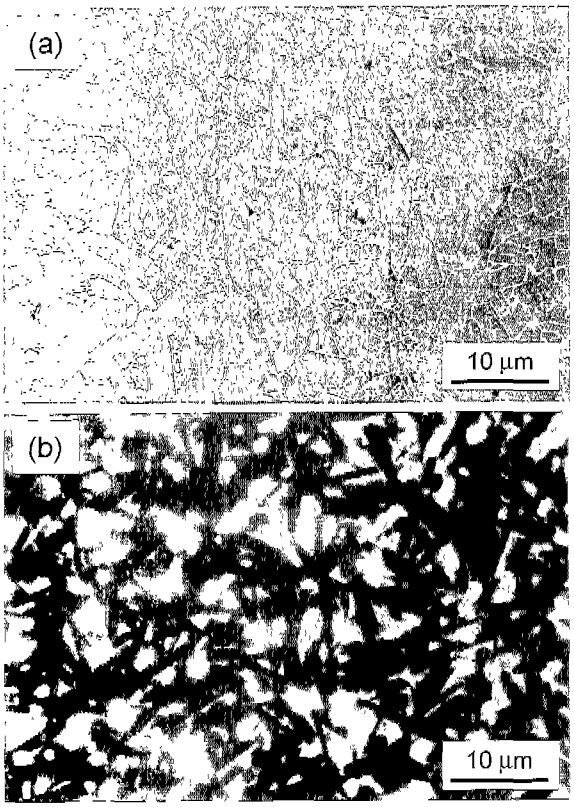

Fig. 1. Typical microstructures of the sintered and annealed materials: (a) monolithic SiC and (b) SiC-TiC composites.

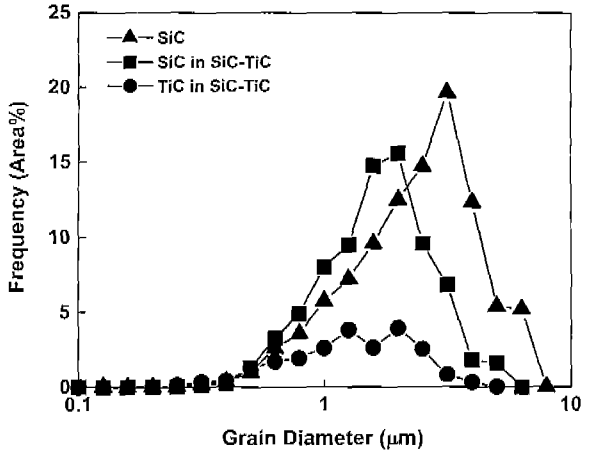

Fig. 2. Grain-diameter distribution of SiC and TiC grains revealed by the relation between grain diameter and areal frequency for monolithic SiC and SiC-TiC composites.

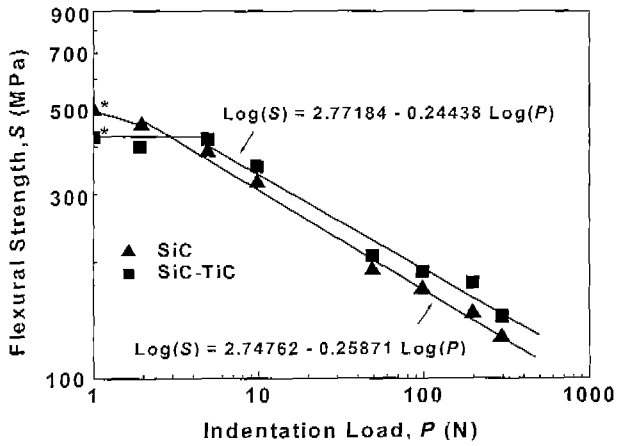

Fig. 3. Plots of strength (S) versus indentation load (P) for monolithic SiC and SiC-TiC composites. The strengths (*) from natural flaws were arbitrarily plotted at P = 1 N.

uted elongated α-SiC grains ("dark") and relatively equiaxed TiC grains ("bright").

As shown in Table 2, β→α phase transformation of SiC was occurred during annealing. The grain growth of SiC grains in both materials have resulted from the overgrowth of β-SiC on α-SiC seeds,[12] because of hot-pressing temperature as low as 1820°C, where β-SiC might have been stable or where the β→α phase transformation might have been very slow. The overgrowth of β-SiC on α-SiC seeds have resulted in α/β composite grains, which we observed in monolithic SiC using high-resolution electron microscopy previously.[16] Strain at the α/β interface may have accelerated the growth of elongated grains.[17] The marked growth of elongated α-SiC grains, thus, is related to the β→α phase transformation of SiC during annealing.[18,19]

Fig. 2 shows the grain-diameter distribution of SiC and TiC grains for monolithic SiC and SiC-30 wt% TiC composites. Monolithic SiC had a unimodal grain-diameter distribution ranging from 0.1-6.3 μm. SiC-30 wt% TiC composites had unimodal diameter distributions for TiC grains ranging from 0.1-4.0 μm and for SiC grains ranging from 0.1-5.0 μm. The aspect ratio of SiC grains was 3.9 for monolithic SiC and 4.7 for SiC-TiC composites. The aspect ratio of TiC grains in SiC-TiC composites was 2.8.

3.2. R-Curve Behavior

The fracture strength versus indentation load for monolithic SiC and SiC-30 wt% TiC composites is shown in Fig. 3. The unindented strengths of both specimens were arbitrarily plotted at P = 1 N. Every specimen was checked to ensure that fracture was initiated from the indent. Flexural strength for monolithic SiC declined from natural flaws (i.e., unindented strength, 495 MPa) at 1.96 N indentation. In contrast, flexural strength for SiC-TiC composites declined from natural flaws (424 MPa) at 4.9 N indentation. Initially monolithic SiC has about 17% higher strength than SiC-TiC composites. However, after 4.9 N indentation, monolithic SiC loses about 22% of its initial strength, while SiC-TiC composites maintain their initial strength and have a higher strength than monolithic SiC for an equivalent indentation load. This result indicates that the SiC-TiC composites possess improved flaw tolerance in comparison with monolithic SiC. It also suggests that SiC-TiC composites may have a higher fracture resistance than monolithic SiC.

Linear regression was used to obtain the best fit for the data from monolithic SiC and SiC-TiC composites. It showed that slopes of monolithic SiC and SiC-TiC composites in Fig. 3 were 0.25871 and 0.24438, respectively. Griffith materials, which show no rising R-curve behavior, have a slope of 1/3, and R-curve materials have lower slopes.[15] Because the slopes of both materials are less than 1/3, rising R-curve behavior is expected for both materials.

R-curve behavior was estimated from the indentation-strength data in Fig. 3 by assuming that the fracture resistance (K_R) was related to the crack length (c) by a power-law relation, $K_R = k(\Delta c)^m$, as suggested by Krause.[15] k is a constant and m is a constant reflecting the extent of R-curve behavior for the material. The power-law relation is a strictly empirical relation, and is used simply as a means to obtain estimates of the R-curve. Table 3 summarizes the important parameters needed for estimation of the R-curve for monolithic SiC and SiC-TiC composites. The estimated R-curves for monolithic SiC and SiC-30 wt% TiC composites are shown in Fig. 4, where the predicted fracture resistance curves as a function of crack size are given. As shown, both

Table 3. Important Parameters* Defining Fracture Resistance

Material	β	log α	log γ	m
SiC	0.25871	2.75	7.99	0.089
SiC-TiC	0.24438	2.77	7.98	0.107

*Refer to Reference 15.

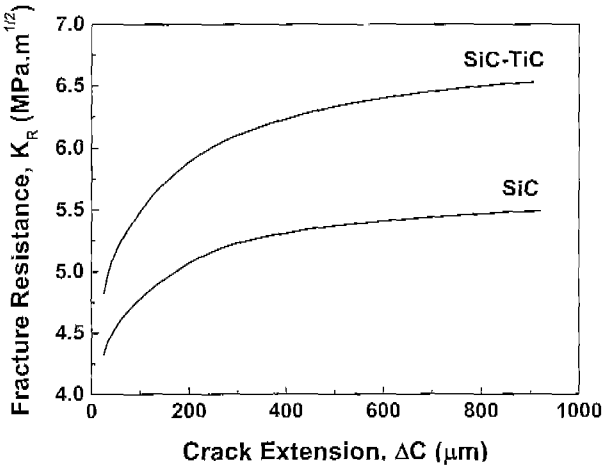

Fig. 4. Estimated R-curves for monolithic SiC and SiC-TiC composites by the indentation-strength method.

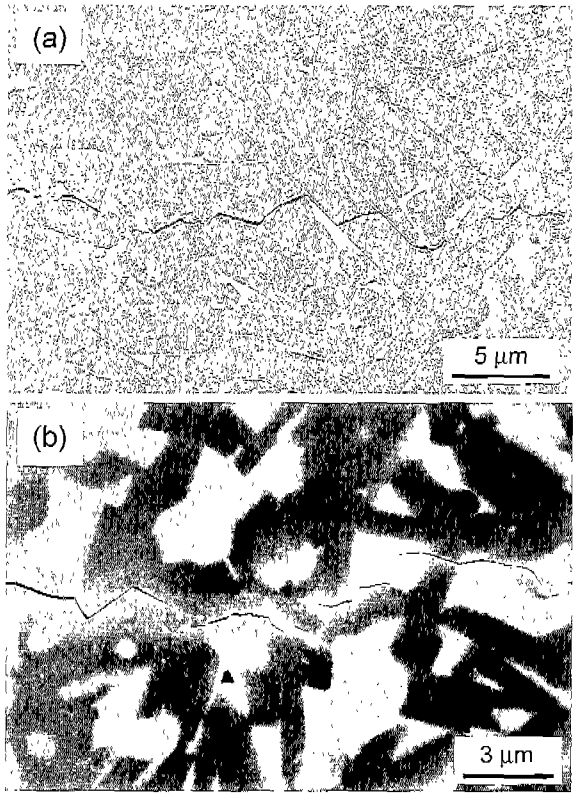

Fig. 5. SEM micrographs of crack paths induced by a Vickers indentation for (a) monolithic SiC and (b) SiC-TiC composites.

materials have rising crack-growth resistance behavior, i.e., R-curves with toughening exponents of m = 0.089 and 0.107 for monolithic SiC and SiC-TiC composites, respectively. The SiC-TiC composites have higher values of K_R than monolithic SiC in the measured crack size range between 25 to 920 μm, as expected from the indentation-results (Fig. 3).

In monolithic SiC with toughened microstructure, a principal source of increased fracture toughness is believed to be crack bridging by elongated grains behind the crack tip.[18-20] As the fracture front advances, the grain bridging sites are left behind and provide a restraining force which must ultimately be overcome for failure to occur. SEM micrographs indicate some evidence of bridging grains in both monolithic SiC and SiC-TiC composites (Fig. 5).

In particulate composites, a principal source of increased fracture toughness is believed to be crack deflection by reinforcing particles ahead of a propagating crack.[21,22] A SEM micrograph indicates some evidence of crack deflection around TiC grains as well as bridging by elongated SiC grains (Fig. 5(b)). An additional source of increased fracture toughness of SiC-TiC composites could be the thermal residual stress caused by the thermal expansion mismatch between SiC and TiC. The developed residual stress around the TiC particle, radial matrix stress (σ_{mr}), can be estimated from the following equation:[22]

$$\sigma_{mr} = (\alpha_p - \alpha_m)\,\Delta T/\{[(1+\nu_m)/2E_m] + [(1-2\nu_p)/E_p]\} \quad (1)$$

where ν is Poission's ratio, ΔT is the temperature difference over which stresses are not relieved by a diffusive process,[23] and the subscripts p and m refer to the particle and matrix, respectively. Taking 7.4×10^{-6}/°C and 4.8×10^{-6}/°C for α_p and α_m, 430 GPa and 420 GPa for E_p and E_m, 0.19 and 0.18 for ν_p and ν_m, respectively, and 800°C for ΔT, the developed radial tensile stress around TiC particles is ~670 MPa. The high tensile stress could be relieved by generating microcracks in the vicinity of TiC. In SiC-TiB_2 and Si_3N_4-TiN composites, which have thermal expansion mismatches similar to those of SiC-TiC composites in this study, stress-induced microcracking due to the residual stresses was reported.[8,9] Therefore, it is inferred that the unrelieved residual stresses around the TiC particles may induce microcracking when external stresses are applied. This stress-induced microcracking forms a process zone around the main crack and partially shields it.[24,25] Further, as demonstrated by models and verified by experiments by Faber *et al.*,[8,24,26] the shielding effect increases with crack extension and contributes to the R-curve behavior.

In a previous work,[13] we observed that the fracture toughness of SiC ceramics increased with increasing the total volume of key grains. Key grain is defined as a grain which plays a key role regarding the toughening behavior of SiC ceramics. In this work, total volume fraction of SiC key grains were 0.607 for monolithic SiC and 0.614 for SiC-TiC composites; i.e., there was no appreciable difference in both materials. Therefore, the greater damage tolerance and higher resistance to crack growth for SiC-TiC composites can be attributed to (i) stress-induced microcracking at heterophase boundaries (SiC/TiC) caused by the thermal expansion mismatch between SiC and TiC, and (ii) some contribution from crack deflection by TiC grains.

4. Conclusions

R-curves for monolithic SiC and SiC-30 wt% TiC composites were obtained using the indentation-strength method.

The results showed a higher resistance to crack growth and better damage tolerance for the SiC-TiC composites, compared to those of the monolithic SiC. The better properties demonstrated by SiC-TiC composites can be attributed to stress-induced microcracking at heterophase boundaries and some contribution from crack deflection by TiC grains.

Acknowledgement

This work was supported by Grant No. 98-0300-06-01-3 from the Basic Research Program of the Korea Science and Engineering Foundation (KOSEF).

REFERENCES

1. K. S. Park, S. W. Lee and J. H. Lee, "R-Curve Behavior of Particulate Composites of Al_2O_3 Containing SiC and ZrO_2: I. Experiment," *J. Kor. Ceram. Soc.*, **37**(4), 359-367 (2000).
2. S. W. Na and J. H. Lee, "R-Curve Behavior of Particulate Composites of Al_2O_3 Containing SiC and ZrO_2: II. Theoretical Analysis," *J. Kor. Ceram. Soc.*, **37**(4), 368-375 (2000).
3. P. F. Becher, "Microstructural Design of Toughened Ceramics," *J. Am. Ceram. Soc.*, **74**(2), 255-269 (1991).
4. B. J. Choi and H. E. Kim, "R-Curve Behavior of Silicon Nitride Ceramic Reinforced with Silicon Carbide Platelets," *J. Am. Ceram. Soc.*, **81**(8), 2191-2193 (1998).
5. Y-W. Kim, M. Mitomo and N. Hirosaki, "R-Curve Behavior of Sintered Silicon Nitride," *J. Mater. Sci.*, **30**, 4043-4048 (1995).
6. S. K. Lee, D. K. Kim and C. H. Kim, "Flaw-tolerance and R-Curve Behavior of Liquid-phase-sintered Silicon Carbides with Different Microstructures," *J. Am. Ceram. Soc.*, **78**(1), 65-70 (1995).
7. J. Y. Kim, H. G. An, Y-W. Kim and M. Mitomo, "R-Curve Behaviour and Microstructure of Liquid-phase Sintered α-SiC," *J. Mater. Sci.*, **35**, 3693-3697 (2000).
8. W. H. Gu, K. T. Faber and R. W. Steinbrech, "Microcracking and R-Curve Behavior in SiC-TiB_2 Composites," *Acta Metall. Mater.*, **40**(11), 3121-3128 (1992).
9. H. J. Choi, K. S. Cho, J. G. Lee and Y-W. Kim, "R-Curve Behavior of Silicon Nitride-titanium Nitride Composites," *J. Am. Ceram. Soc.*, **80**(10), 2681-2684 (1997).
10. H. G. An, Y-W. Kim and J. G. Lee, "Effect of Initial α-phase Content of SiC on Microstructure and Mechanical Properties of SiC-TiC Composites," *J. Europ. Ceram. Soc.*, **21**, 93-98 (2001).
11. Y-W. Kim, S. G. Lee and Y. I. Lee, "Pressureless Sintering of SiC-TiC Composites with Improved Fracture Toughness," *J. Mater. Sci.*, **35**, 5569-5574 (2000).
12. Y-W. Kim, M. Mitomo and H. Hirotsuru, "Microstructural Development of Silicon Carbide Containing Large Seed Grains," *J. Am. Ceram. Soc.*, **80**(1), 99-105 (1997).
13. S. G. Lee, Y-W. Kim and M. Mitomo, "Relationship between Microstructure and Fracture Toughness of Toughened Silicon Carbide Ceramics," *J. Am. Ceram. Soc.*, **84**(6), 1347-1353 (2001).
14. N. Hirosaki, Y. Akimune and M. Mitomo, "Quantitative Analysis of Microstructure of Self-reinforced Silicon Nitride Ceramics," *J. Ceram. Soc. Jpn.*, **101**(11), 1239-1243 (1993).
15. R. F. Krause, "Rising Fracture Toughness From the Bending Strength of Indented Alumina Beams," *J. Am. Ceram. Soc.*, **71**(5), 338-343 (1988).
16. Y-W. Kim, M. Mitomo and H. Hirotsuru, "Microstructure and Polytype of *In Situ*-toughened Silicon Carbide," *Kor. J. Ceram.*, **2**(3), 152-156 (1996).
17. L. U. Ogbuji, T. E. Mitchell, A. H. Heuer and S. Shinozaki, "The Transformation in Polycrystalline SiC: IV, A Comparison of Conventionally Sintered, Hot-pressed, Reaction-sintered, and Chemically Vapor Deposited Samples," *J. Am. Ceram. Soc.*, **64**(2), 100-105 (1981).
18. Y-W. Kim, M. Mitomo, H. Emoto and J. G. Lee, "Effect of Initial α-phase Content of SiC on Microstructure and Mechanical Properties of Sintered Silicon Carbide," *J. Am. Ceram. Soc.*, **81**(12), 3136-3140 (1998).
19. H. K. Sung, K. S. Cho, N. J. Park, H. J. Choi and J. G. Lee, "A Study on Texture Development in Liquid-phase Sintered Silicon Carbide," *J. Kor. Ceram. Soc.*, **37**(4) 320-326 (2000).
20. Y-W. Kim, M. Mitomo and H. Hirotsuru, "Grain Growth and Fracture Toughness of Fine-grained Silicon Carbide Ceramics," *J. Am. Ceram. Soc.*, **78**(11), 3145-3148 (1995).
21. K. T. Faber and A. G. Evans, "Crack Deflection Process-I. Theory," *Acta Metall.*, **31**(4), 567-576 (1983).
22. G. C. Wei and P. F. Becher, "Improvements in Mechanical Properties in SiC by the Addition of TiC Particles," *J. Am. Ceram. Soc.*, **67**(8), 571-574 (1984).
23. A. G. Evans and T. G. Landon, "Structural Ceramics," *Prog. Mater. Sci.*, **21**(3-4), 196-201 (1976).
24. A. G. Evans and K. T. Faber, "Crack Growth Resistance of Microcracking Brittle Materials," *J. Am. Ceram. Soc.*, **67**(4), 255-260 (1984).
25. J. W. Hutchinson, "Crack Tip Shielding by Micro-cracking in Brittle Solids," *Acta Metall.*, **35**(7), 1605-1619 (1987).
26. G. D. Bowling, K. T. Faber and R. G. Hoagland, "Computer Simulations of R-Curve Behavior in Microcracking Materials," *J. Am. Ceram. Soc.*, **70**(11), 849-854 (1987).